MODELLING OF DIRECT REDUCTION IN A ROTARY HEARTH FURNACE FOR METALLURGICAL DUST RECYCLING: MODEL DEVELOPMENT

Yuliang WU[1,2], Yansong SHEN[2*], Aibing YU[2], Zeyi JIANG[3], Xinxin ZHANG[4] and Qingguo XUE[1]

[1] School of Metallurgical and Ecological Engineering, University of Science and Technology Beijing, Beijing 100083, CHINA
[2] Department of Chemical Engineering, Monash University, Clayton, VIC 3800, AUSTRALIA
[3] Beijing Engineering Research Center for Energy Saving and Environmental Protection, University of Science and Technology Beijing, Beijing 100083, CHINA
[4] Beijing Key Laboratory for Energy Saving and Emission Reduction of Metallurgical Industry, University of Science and Technology Beijing, Beijing 100083, CHINA

*Corresponding author, E-mail address: yansong.shen@monash.edu

ABSTRACT

The metallurgical dusts can be recycled in rotary hearth furnaces (RHF) by means of direct reduction after adding into carbon-based composite pellets. While iron resources in the dust are recycled, heavy and alkali metals including Zn, Pb, K and Na, harmful for blast furnace operation, can also be separated and recycled. However, there is a lack of understanding on direct reduction of carbon-based pellets under industrial-scale RHF conditions in the past. This paper reports a model of direct reduction in a RHF for metallurgical dust treatment. The integrated model includes three mathematical models and one experimental model, including a 3D CFD model of gas flow and heat transfer in RHF, a 1D CFD model of direct reduction inside a pellet, an energy/mass equilibrium model, and a reduction experiment using a Si-Mo furnace. The model is validated by comparing the simulation results with measurements. The model is then used for investigating the effects of key variables on pellet's behaviours in direct reduction and zinc removal behaviours under industrial RHF conditions. It is shown that temperature and atmosphere around pellets play an important role in determining pellet quality especially for iron metallization.

NOMENCLATURE

c_p specific heat at constant pressure of furnace gas
$c_{p,p}$ specific heat at constant pressure of pellet
$C_{i\varepsilon}$ constant of k-ε model, i=1-3
$D_{e,k}$ diffusion coefficient of gas species k inside pellet
E total energy of furnace gas
Ea_i activation energy of reaction i
G_b production of turbulent k by buoyancy
G_k production of turbulent k by velocity gradient
h internal energy of furnace gas
$h_{e,k}$ convective mass transfer coefficient of gas species k on pellet surface
ΔH_i heat of reaction i
k turbulent kinetic energy
$K_{0,i}$ pre-exponential constant in rate constant of reaction i
$M_{s,k}$ molar mass of solid species k
$M_{s,R}^i$ molar mass of solid reactant of reaction i
n_{gr} number of grain inside pellet per unit volume
P pressure of furnace gas
P_0 total pressure of gas inside pellet

r radial coordinate of pellet
r_{gr0} initial radius of grain inside pellet
R gas constant
$R_{e,k}$ reynolds number of gas species k
R_p equivalent radius of pellet
$R_{v,i}$ local rate per unit volume of reaction i
sf_{gr} shape factor of grain inside pellet
$S_{c,k}$ schmidt number of gas species k
S_h heat sources
T_f furnace temperature
T_0 temperature of feeding pellet
v_i, v_j velocity components of furnace gas
$\Delta X_{g,k}^i$ variation ratio of gas species k in reaction i
$\Delta X_{s,k}^i$ variation ratio of solid species k in reaction i

δ_{ij} kronecker delta
ε turbulent dissipation rate
ε_p comprehensive emissivity of pellet surface
λ_{eff} effective thermal conductivity of pellet
λ_g thermal conductivity of gas inside pellet
λ_s thermal conductivity of solid inside pellet
μ viscosity of furnace gas
μ_t turbulent viscosity of furnace gas
ρ density of furnace gas
$\rho_{g,k}$ molarity of gas species k inside pellet
$\rho_{g0,k}$ initial molarity of gas species k inside pellet
$\rho_{gf,k}$ molarity of gas species k around pellet
$\rho_{g,R}^i$ molarity of gas reactant of reaction i
$\rho_{g,R}^{eq,i}$ equilibrium molarity of gas reactant of reaction i
ρ_p apparent density of pellet
$\rho_{s,k}$ molarity of solid species k
$\rho_{s0,k}$ initial molarity of solid species k
$\rho_{sr,k}$ density of solid species k
$\rho_{s,R}^i$ molarity of solid reactant of reaction i
$\rho_{sr,R}^i$ density of solid reactant of reaction i
σ_k turbulent prandtl number for k
σ_ε turbulent prandtl number for ε
ϕ porosity of pellet

INTRODUCTION

Steel industry generates a significant amount of dust waste (usually called metallurgical dusts), approximately 8%-

12% of the steel output, from sintering processes, pelletizing processes, blast furnaces, oxygen converters and rolling processes (World Steel Association, 2010). For example, China's crude steel output is 0.8 billion tons in 2014, that is, nearly 100 million tons dusts were generated (World Steel Association, 2014). Typically, metallurgical dusts contain 30%-70% iron, as well as other elements such as C, Zn, Pb, K or Na. In the past, these dusts were mainly recycled by sintering for recovering iron, which leads to a damage in sinter quality and also has a negative effect on blast furnace operation due to zinc accumulation in iron circle (Senk et al., 2006; Cantarino et al., 2012).

Rotary hearth furnace (RHF) was originally used for rolling steel heating, and recently proposed for recycling metallurgical dusts due to its efficient performance in reducing iron oxides into metal Fe and removing Zn, Pb, K and Na from dusts (Xiong and Dai, 2012). In this process, different metallurgical dusts, added with adhesive bond and carbon-containing powder for an appropriate C/O ratio, are well-mixed and then compressed into cold pellets using a briquetting machine. After drying, the prepared pellets are fed into the RHF for direct reduction. During direct reduction process, metal Fe is reduced from iron oxides; zinc vapour reduced from ZnO diffuses out of pellets and then is re-oxidized into solid particles of oxides; PbO is removed by volatilization of both PbO itself and its reduced product Pb; removal of K and Na, existing as chlorides, is attributed to volatilization of KCl and NaCl. Metallized pellets are charged into blast furnace after cooling; Zn, Pb, K and Na products are collected in secondary dusts by flue gas treating system for further use (Oda et al., 2006).

Although RHF has been used in treating and recycling metallurgical dusts for years, there are still some technical issues, such as undesired gas flow near pellet feeding/discharging zones and unstable iron metallization. This is mainly related to the complexity and instability in direct reduction process compared to rolling heating process by RHF.

In recent decades, the carbon-based direct reduction process has been studied by both experiment and numerical simulation. For example, various experimental studies have been conducted by TGA, XRD, EDS, etc. (Huang and Lu, 1993; Wei et al., 2011; Xia et al., 2015; Peng et al., 2009). However, these studies are expensive and cannot sufficiently describe behaviours of briquettes in practice. On the other hand, several mathematical models were also developed for simulating direct reduction process in carbon-based composite pellets. For example, Coetsee et al. (2002) developed a non-isothermal and non-isobaric mathematical model for investigating rate-limiting steps for reduction in magnetite-coal pellets. They found that heat transfer is not the rate-limiting step. Donskoi et al. (2001) developed a model of direct reduction in a highly swelling iron ore-coal char composite pellet and found that the swelling of the composite pellet has some effect on the reduction process and this effect increases with the increase of initial pellet size. Fortini et al. (2005) developed a model of direct reduction of composite pellets, in which effects of pellet shrinkage were considered. Sun and Lu (2009; 1999; 1993) included mass/heat transfer rate and reaction rate simultaneously in his kinetics model of direct reduction in ore-coal composite pellets. Wu et al. (2013) established a

mathematical model of direct reduction of composite pellets made of metallurgical dust to study the behaviour of iron metallization and dezincification in the composite pellets. Liu et al. (2014) established a combined model for investigating the effects of C/O mole ratio in the feed pellets on reduction kinetics and heat/mass transfer as well as combustion processes in a pilot-scale RHF. However, the abovementioned models were mainly developed under lab or pilot scale. There is still a lack of understanding on direct reduction of carbon-based pellets under industrial-scale.

This paper reports a model of direct reduction in RHF for metallurgical dust recycling. The integrated model includes three mathematical models and one experimental model, including a 3D CFD model of gas flow and heat transfer in an industrial-scale RHF, a 1D CFD model of direct reduction inside a composite pellet, an energy/mass equilibrium model, and a reduction experiment using a Si-Mo furnace. The model is validated by experimental and reported data, and then used for investigating pellet's behaviours in direct reduction and zinc removal under industrial RHF conditions.

MODEL DESCRIPTION

The schematic of industrial-scale RHF is shown in Figure 1. The inner and outer diameters of the chamber are 27 and 37 m, respectively. The furnace is divided into five sections (332°): preheating (54°), reducing I (78°), reducing II (78°), reducing III (60°) and soaking sections (62°). The composite pellets with equivalent diameter of 25 mm are placed in a single layer on furnace hearth.
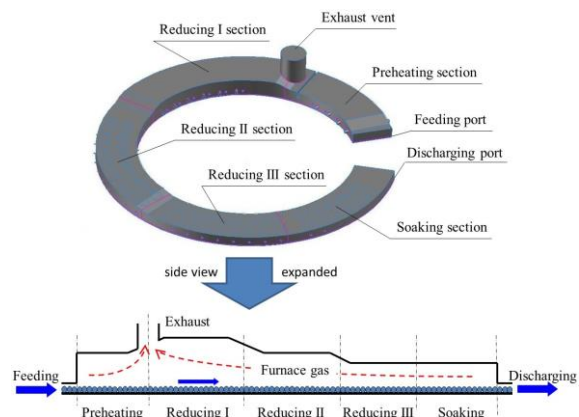
Figure 1: Schematic of an industrial-scale RHF.

Compared with RHF for rolling heating, the RHF for direct reduction is more complicated, in two aspects: 1) the overall reaction in composite pellets during direct reduction is endothermic, thus more energy is required from furnace chamber; 2) significant amounts of CO is generated from reducing pellets, and could be used as fuel supplementary by combustion (usually called secondary combustion). Therefore, the interactions between behaviours in furnace chamber and inside pellets should be considered in its model studies.

The solution procedure of the integrated model is shown in Figure 2. Firstly, the temperature change and reactions of composite pellets in each RHF section are initially estimated based on the data from reduction experiment using a Si-Mo furnace, and are then used to calculate the

2

RHF section-related parameters by using energy and mass equilibrium model, including the quantity of generated CO and required secondary air to burn them out, the quantity of required gas fuel and primary air to secure energy supplies, as well as the quantity and components of generated flue gas from each RHF section. Secondly, these RHF section-related parameters are treated as boundary conditions and heat/mass sources for CFD model to calculate gas flow and heat transfer in RHF chamber including temperature, flow and pressure field of furnace gas. Thirdly, these thermal data in RHF chamber are provided to CFD model of direct reduction inside one pellet as boundary conditions for simulating temperature, components and technical indexes of composite pellets under these conditions. Finally, the results are compared with experimental data from the Si-Mo furnace. On the basis, calculation conditions of the energy and mass equilibrium model are updated for further iterations until convergence. The sub-models will be described in details.
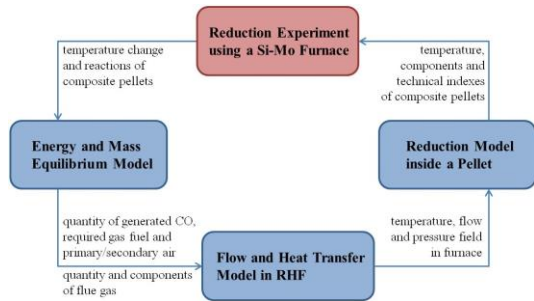
Figure 2: Solution procedure of the integrated model.

Flow and Heat Transfer Model in RHF

The CFD part of this model is based on a CFD commercial software ANSYS-Fluent. Standard k-ε model and P1 model are used for modelling turbulent flow and radiative heat transfer, respectively. Pressure and velocity are coupled by SIMPLE algorithm, and the first order upwind is applied for discretization.

Section	Gas Fuel Burners	Secondary Air Nozzles
Preheating	side (6 outer, 4 inner)	side (6 outer, 4 inner)
Reducing I	side (10 outer, 6 inner)	side (10 outer, 6 inner)
Reducing II	top (11 pairs)	side (11 outer, 8 inner)
Reducing III	top (9 pairs)	side (8 outer, 5 inner)
Soaking	top (7 pairs)	side (2 outer, 2 inner)

Table 1: Arrangement of burners and secondary air nozzles.

Assumptions

In order to improve the efficiency of simulation, some assumptions are made: 1) the single layer of pellets on RHF hearth is simplified as one flat plate layer of porous media; 2) CO generated from the pellets during direct reduction and heat required for heating pellets and chemical reactions are regarded as mass source and energy sink of the pellet layer, respectively; 3) the combustion heat of gas fuel and generated CO is treated as enthalpy of combustion product. The arrangement of burners and

secondary air nozzles (used for secondary combustion of generated CO) is shown in Table 1.

Governing Equations

(1) Continuity equation:

$$\frac{\partial \rho}{\partial \tau} + \frac{\partial}{\partial x_i}(\rho v_i) = 0 \tag{1}$$

(2) Momentum equation:

$$\rho \frac{D v_i}{D \tau} = -\frac{\partial P}{\partial x_i} + \frac{\partial}{\partial x_j}\left(-\rho \overline{v_i' v_j'}\right) + \frac{\partial}{\partial x_j}\left[\mu\left(\frac{\partial v_i}{\partial x_j} + \frac{\partial v_j}{\partial x_i} - \frac{2}{3}\delta_{ij}\frac{\partial v_1}{\partial x_1}\right)\right] \tag{2}$$

(3) k-ε equations:

$$\rho \frac{Dk}{D\tau} = \frac{\partial}{\partial x_i}\left[\left(\mu + \frac{\mu_t}{\sigma_k}\right)\frac{\partial k}{\partial x_i}\right] + G_k + G_b - \rho\varepsilon \tag{3}$$

$$\rho \frac{D\varepsilon}{D\tau} = \frac{\partial}{\partial x_i}\left[\left(\mu + \frac{\mu_t}{\sigma_\varepsilon}\right)\frac{\partial \varepsilon}{\partial x_i}\right] + C_{1\varepsilon}\frac{\varepsilon}{k}(G_k + C_{3\varepsilon}G_b) - C_{2\varepsilon}\rho\frac{\varepsilon^2}{k} \tag{4}$$

(4) Energy equations:

$$\frac{\partial}{\partial \tau}(\rho E) + \frac{\partial}{\partial x_i}[v_i(\rho E + P)] = \frac{\partial}{\partial x_i}\left[\frac{k_t}{c_p}\frac{\partial E}{\partial x_i}\right] + S_h \tag{5}$$

$$E = h - \frac{P}{\rho} + \frac{u_i^2}{2} \tag{6}$$

Boundary Condition

The boundary conditions are mainly calculated by energy and mass equilibrium model. The momentum and energy inlet of burners are respectively specified as the flow of flue gas and the theoretical flame temperature of gas fuel. For the secondary air nozzles, these two inlets are respectively set as the flow and reheating temperature of secondary air. The pressure boundary conditions are specified in feeding/discharging ports and exhaust vent. The furnace wall is treated as no-slip with a constant heat loss flux.

Reduction Model inside a Pellet

Assumptions

Some assumptions are made for one single composite pellet as follows: 1) the ellipsoidal pellet is regarded as spherical with constant diameter, thus the heat and mass transfer inside the pellet is one dimensional along the radial direction; 2) gas-solid chemical reactions are carried out in isothermal system; 3) total pressure within the pellet is constant, so the viscous gas flow through connected pores caused by pressure gradient was neglected.

Chemical Reactions

The carbon-based direct reductions occur mainly through gaseous intermediates CO and CO_2. Chemical reactions considered in this model are presented as follows:

(1) Carbon gasification:

$$C + CO_2 = 2CO \tag{7}$$

(2) Iron oxide reductions:

$$3Fe_2O_3 + CO = 2Fe_3O_4 + CO_2 \tag{8}$$

$$Fe_3O_4 + 4CO = 3Fe + 4CO_2 \tag{9}$$

$$Fe_3O_4 + CO = 3FeO + CO_2 \tag{10}$$

$$FeO + CO = Fe + CO_2 \tag{11}$$
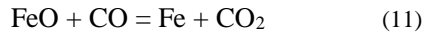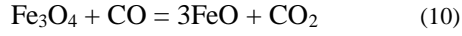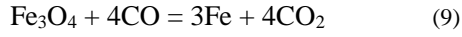
(3) Zinc oxide reduction:

$$ZnO + CO = Zn + CO_2 \tag{12}$$

Governing Equations

(1) Energy conservation equation:

$$\rho_p c_{p,p} \frac{\partial T}{\partial \tau} = \frac{1}{r^2} \frac{\partial}{\partial r}\left(r^2 \lambda_{eff} \frac{\partial T}{\partial r}\right) + \sum_i R_{v,i} \cdot \Delta H_i \tag{13}$$

Where λ_{eff} and ΔH_i are calculated using the following relationship (Donskoi, 2001):

$$\lambda_{eff} = \frac{2}{3}\left[\phi \cdot \lambda_g^{-1} + (1-\phi) \cdot \lambda_s^{-1}\right]^{-1}$$
$$+ \frac{1}{3}\left[\phi \cdot \lambda_g + (1-\phi) \cdot \lambda_s\right] \tag{14}$$

$$\Delta H_i = a \cdot 10^3 + bT + c \cdot 10^{-3}T^2 + d \cdot 10^{-6}T^3 \tag{15}$$

(2) Mass conservation equation for solid species:

$$\frac{\partial \rho_{s,k}}{\partial \tau} = \sum_i R_{v,i} \cdot \Delta X_{s,k}^i \tag{16}$$

(3) Mass conservation equation for gas species:

$$\frac{\partial(\phi \rho_{g,k})}{\partial \tau} = \frac{1}{r^2}\frac{\partial}{\partial r}\left[r^2 D_{e,k}\frac{(\phi \rho_{g,k})}{\partial r}\right] + \sum_i R_{v,i} \cdot \Delta X_{g,k}^i \tag{17}$$

Where $D_{e,k}$ is defined as function of temperature (Wu, 2013).

(4) Kinetic expression of gas-solid reactions:

Based on the porous particle model (Hua, 2003), local gas-solid reactions take place on the surface of grains when the partial pressure of reactant gas exceeds its equilibrium value. Reaction rate can be calculated by:

$$R_{v,i} = sf_{gr} \cdot n_{gr} \cdot 4\pi r_{gr0}^2 \left(\frac{\rho_{s,R}^i \cdot M_{s,R}^i / \rho_{sr,R}^i}{\sum_k \rho_{s0,k} \cdot M_{s,k} / \rho_{sr,k}}\right)^{2/3} \tag{18}$$
$$\cdot K_{0,i} \cdot e^{-\frac{Ea_i}{RT}} \cdot P_0 \cdot \frac{\rho_{g,R}^i - \rho_{g,R}^{eq,i}}{\sum_k \rho_{g,k}}$$

Where sf_{gr}, n_{gr} and r_{gr0} are obtained from the measurements of metallurgical dusts which are used to make composite pellets.

Initial and Boundary Conditions

The boundary conditions are calculated by flow and heat transfer model in RHF.

(1) Energy conservation equation:

$$T\big|_{\tau=0} = T_0, \left(0 \le r \le R_p\right) \tag{19}$$

$$\frac{\partial T}{\partial r}\bigg|_{\tau>0} = 0, (r = 0) \tag{20}$$

$$\lambda_{eff}\frac{\partial T}{\partial r}\bigg|_{\tau>0} = \varepsilon\sigma\left[T_f^4 - \left(T\big|_{r=R_p}\right)^4\right](r = R_p) \tag{21}$$

Where ε is related to emissivity of pellet surface, emissivity of furnace gas, furnace structures, and radiation shape factor between pellets and furnace lining.

(2) Mass conservation equation for solid species:

$$\rho_{s,k}\big|_{\tau=0} = \rho_{s0,k}, \left(0 \le r \le R_p\right) \tag{22}$$

(3) Mass conservation equation for gas species:

$$\rho_{g,k}\big|_{\tau=0} = \rho_{g0,k}, \left(0 \le r \le R_p\right) \tag{23}$$

$$\frac{\partial \rho_{g,k}}{\partial r}\bigg|_{\tau>0} = 0, (r = 0) \tag{24}$$

$$D_{e,k}\frac{\partial \rho_{g,k}}{\partial r}\bigg|_{\tau>0} = h_{e,k}\left(\rho_{gf,k} - \rho_{g,k}\big|_{r=R_p}\right), (r = R_p) \tag{25}$$

Where $h_{e,k}$ is calculated according to Steinberger empirical formula, used for describing gas flow around a single sphere as below:

$$h_{e,k} = 2 + 0.552 \cdot R_{e,k}^{0.53} \cdot S_{c,k}^{1/3} \tag{26}$$

An in-house code in C# language is developed to solve this pellet model.

Energy and Mass Equilibrium Model

The energy and mass equilibrium model, based on each RHF section, includes three parts: combustion calculation, material balance calculation and heat balance calculation. The function of material balance calculation is to calculate the quantity of CO generated from pellets in each RHF section. Combustion calculation is then employed for obtaining the quantity of air required to burn CO out, as well as the heat obtained during its secondary combustion.

Heat balance calculation is the core of equilibrium model. It is used to calculate the required quantity of gas fuel provided into each RHF section for heating pellets and reducing metal oxides. Flow and components of flue gas can also be obtained by combustion calculation, supplied to the flow and heat transfer model in RHF as boundary conditions.

Reduction Experiment using a Si-Mo Furnace

As it is difficult to measure reduction indexes in a practical RHF production, a direct reduction experiment of one single dust-made composite pellet in Si-Mo furnace is conducted (Figure 3). After drying for 2 h, the composite pellet was put in a cradle made of Fe-Cr-Mo wires. The cradle was kept at 1000°C in the Si-Mo furnace for 4 min, and then kept at 1250°C for another 24 min while the composition of pellet was measured every 3 min. The flow rate of nitrogen as protection gas was set at 5.0 L/min. After a given time, the pellet was taken to inert gases to avoid re-oxidation. Then, the rates of iron metallization and dezincification were obtained by chemical analysis.
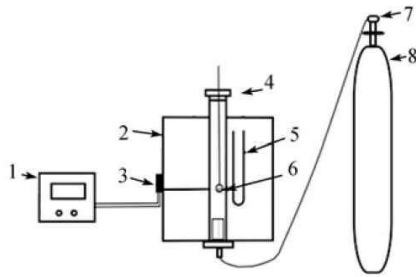
Figure 3: Schematic diagram of direct reduction experimental: 1 temperature controller; 2 Si-Mo furnace; 3 thermocouple; 4 furnace cover; 5 silicon molybdenum rod; 6 sample and cradle; 7 flowmeter; 8 nitrogen.

MODELS VALIDATION

The pellet reduction model is validated by experimental data of the Si-Mo Furnace as shown in Table 2. The results calculated by the flow and heat transfer model in RHF are also compared with reported data (Liu et al., 2014) as shown in Table 3. It can be shown that there is a reasonable agreement between the model predictions and measurements.

Time		Iron metallization (%)	Dezincification (%)
4 min	Calculated	8.0	3.3
	Measured	7.3	3.7
	Error (%)	9.4	11.3
10 min	Calculated	33.8	58.4
	Measured	37.9	58.0
	Error (%)	10.7	0.6
16 min	Calculate	67.2	94.7
	Measured	63.4	97.1
	Error (%)	5.9	2.4
22 min	Calculated	78.9	99.9
	Measured	77.6	99.0
	Error (%)	1.7	1.0

Table 2: Comparison of pellet behaviours between model predictions and experimental data at furnace temperature of 1250°C.

Item		Preheating Section	Reducing II Section	Soaking Section
Furnace Temperature (K)	Calculated	1448	1543	1446
	Measured	1282	1533	1532
	Error (%)	11.5	0.6	6.0
Furnace Pressure (Pa)	Calculated	-6.8	-	-
	Measured	-7.5	-	-
	Error (%)	9.3	-	-

Table 3: Comparison of RHF thermal states between model predictions and reported data.

SIMULATION CONDITIONS

The composite pellet is made of several metallurgical dusts from a steel plant, including fabric filter dust/trough dust from blast furnace, fine ash/coarse ash/OG sludge/surrounding dust from converter, dust from electric cooker, and sludge from rolling process. Table 4 shows the chemical composition of the composite pellet. The equivalent diameter, porosity and preheating temperature of the composite pellet are 25 mm, 0.35 and 343 K, respectively. The composition of coke oven gas, employed as gas fuel of RHF, is shown in Table 5. The preheating temperature of secondary air is 773 K. The residence time of pellets in RHF is 20 min.

Fe	FeO	Fe_2O_3	C	ZnO
3.2	21.9	31.0	11.3	1.5
SiO_2	CaO	MgO	Al_2O_3	S
2.7	6.8	1.5	1.6	0.6

Table 4: Chemical composition of composite pellet made of metallurgical dusts.

H_2	CO	CH_4	C_2H_4	CO_2	N_2	O_2
56.0	6.0	26.0	3.0	3.0	5.5	0.5

Table 5: Chemical composition of coke oven gas.

RESULTS AND DISCUSSION

Furnace Temperature and Pellet Behaviours

Figure 4 and Figure 5 show the temperature distribution of furnace gas in RHF and pellet behaviours (including temperature rise, direct reduction and zinc removal) under this in-furnace condition. It can be shown that the highest furnace temperature appears in reducing II section, ~ 1350°C, and then followed by reducing I section, reducing III section, preheating section and soaking section. This furnace temperature distribution is reasonable to direct reduction process for two reasons: 1) more energy for reducing metal oxide and gasifying carbon are required in reducing sections; 2) heating pellets rapidly in preheating section is favourable for avoiding burning loss of carbon inside pellets, which can then be used further for reduction. It is also shown from Figure 4 that the surface temperature of the pellet reaches nearly 1000°C by the end of preheating section, but the core temperature is only 300°C, along with the maximum temperature difference at this stage. For carbon-based direct reduction process, carbon gasification is the key reaction to provide gas reducing agent CO, and its initial temperature is about 900°C. One can find from Figure 5 that the rate of iron metallization and zinc removal start to increase in reducing I section, and then rise faster in reducing II section, where the core temperature of pellet has just reached 900°C. Figure 5 also shows that the final zinc removal rate is higher than

iron metallization, 90.89% vs. 74.56%. This is because: 1) the ZnO reduction has better thermodynamic condition and higher reaction rate; 2) the iron oxides are reduced step by step in the order of Fe_2O_3, Fe_3O_4 and FeO to Fe, but the ZnO reduction is in one step.
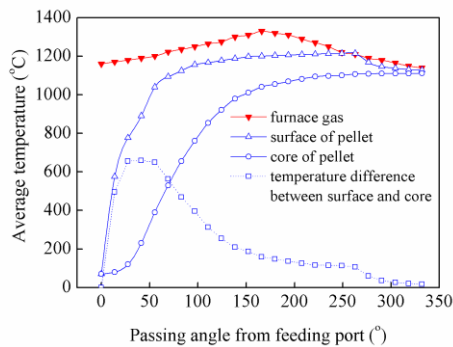
Figure 4: Temperature distribution of furnace gas and reducing pellets in RHF along lengthwise direction.
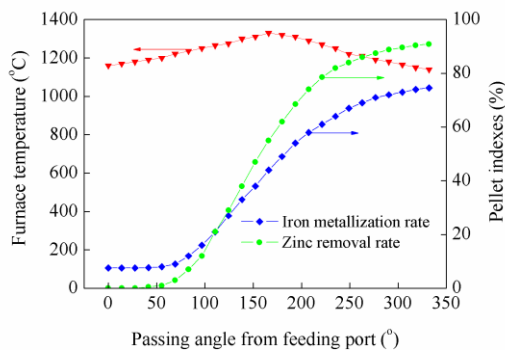
Figure 5: Variation of pellets in iron metallization and dezincification under RHF conditions.

Effect of Furnace Temperature and Atmosphere on Pellet Indexes

In order to identify the key factors on direct reduction and zinc removal, the effects of several key operational variables on the final indexes of discharged pellets are investigated. Figure 6 shows the effect of furnace temperature on iron metallization and dezincification. The in-furnace temperature distribution in Figure 5 is regarded as base case, and other three cases are separately -100°C, -50°C and +50°C of the base case. It can be found that final indexes of both iron metallization and zinc removal are greatly affected by furnace temperature. A temperature drop of 100°C can lead to a drop in these two indexes by approximately 15%. This is because the direct reduction in composite pellets is a strong endothermic process, especially for the carbon gasification, which translates CO_2 into CO constantly for gas-solid reduction.

Figure 7 shows the effect of furnace atmosphere on final indexes of discharged pellets. It is shown that the final iron metallization increases significantly with the rise of CO volume fraction around pellets during their reduction. This is because the iron oxides cannot be reduced by CO if the ratio of $CO/(CO+CO_2)$ is less than its equilibrium value (approximately 60~70%) under local temperature. This result is also consistent with the mechanism of carbon-based direct reduction process. The CO generated from a reducing pellet can form a protective covering layer

of reductive atmosphere around the pellet surface, which makes the direct reduction go smoothly. That is also reason responsible for the result that the carbon-containing pellet can be reduced in oxidative atmosphere. However, if the CO covering atmosphere around the pellet is damaged to some extent, such as blown thinner by oxidative furnace gas with high velocity, the reduction of iron oxide will be slowed down. The result also shows that the fluctuation in CO volume fraction around the pellet has less impact on the final dezincification rate. This is because the equilibrium ratio of $CO/(CO+CO_2)$ for ZnO reduction is proportional to the partial pressure of gas Zn, and the zinc oxide in dust composite pellet is very low, generally less than 5%.
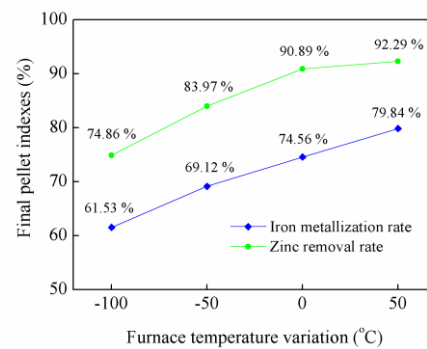
Figure 6: Effect of furnace temperature on final iron metallization and dezincification of pellets in RHF.
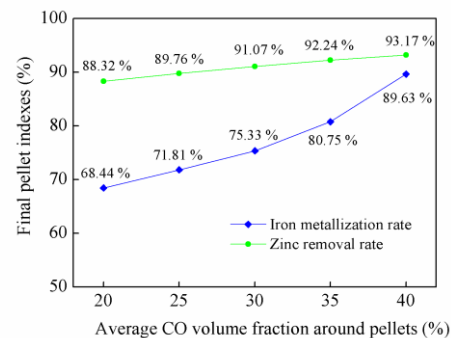
Figure 7: Effect of furnace atmosphere on final iron metallization and dezincification of pellets in RHF.

CONCLUSION

An integrated model is developed for describing direct reduction and zinc removal process of carbon-based composite pellets under industrial-scale RHF conditions, including three mathematical models and one experimental model. The interactions between furnace state and pellet behaviours are considered. The model was validated by the measurements from experiment and literature. The effects of furnace temperature and gas atmosphere around pellet particles on pellet behaviours in aspects of iron metallization and zinc removal are investigated. The following conclusions were obtained.

1) The surface and core temperature of the pellets are increased to 900~1000°C (the initial temperature of carbon gasification) until the end of preheating and reducing I section respectively. The rate of iron

metallization and zinc removal starts to increase in reducing I section, and rise faster in reducing II section.

2) The final zinc removal rate is higher than iron metallization by approximately 15% due to better thermodynamic and kinetics conditions of one-step ZnO reduction, compared with multi-step reduction of iron oxides.

3) Furnace temperature and CO volume fraction around the pellets play an important role in determining final indexes of discharged pellets especially iron metallization. A drop in furnace temperature by 100°C or in CO volume fraction by 10% can lead to drop in final iron metallization by nearly 15% and 10%, respectively.

REFERENCES

WORLD STEEL ASSOCIATION, (2010), "Steel industry by-products", *World Steel Association Publishers*, 147-150.

WORLD STEEL ASSOCIATION, (2014), "Steel statistical yearbook 2014", *World Steel Association Publishers*, 2-3.

SENK, D., GUDENAU, H.W., GEIMER, S. and GORBUNOVA, E., (2006), "Dust injection in iron and steel metallurgy", *ISIJ Int.*, **46(12)**, 1745-1751.

CANTARINO, M.V., FILHO, C.C. and MANSUR, M.B., (2012), "Selective removal of zinc from basic oxygen furnace sludges", *Hydrometall.*, 111-112, 124-128.

XIONG, H.W. and DAI, Y.D., (2012), "Significance for resource comprehensive utilization of rotary hearth furnace direct reduction in steel industry and analysis of its developing prospects", *Energ. China*, **34(2)**, 5-7.

ODA, H., IBAXAKI, T. and TAKAHASHI, M., (2002), "Dust recycling technology by the rotary hearth furnace", *Nippon Steel. Tech. Rep.*, **86**, 30-34.

HUANG, B.H. and LU, W.K., (1993), "Kinetics and mechanisms of reactions in iron ore/coal composites", *ISIJ Int.*, **33(10)**, 1055-1061.

WEI, R.F., LI, J.X., LI, J.M., LONG, H.M., WANG, P., GAO, G. and LIN, G.P., (2011), "Reduction kinetics of carbon-containing pellets made of dust and sludge under weak oxidizing atmosphere", *Chin. J. Process Eng.*, **11(3)**, 429-435.

XIA, L.G., MAO, R., ZHANG, J.L., XU, X.N., WEI, M.F. and YANG, F.H., (2015), "Reduction process and zinc removal from composite briquettes composed of dust and sludge from a steel enterprise", *Int. J. Miner. Metall. Mater.*, **22(2)**, 122-131.

PENG, C., ZHANG, F.L., LI, H.F. and GUO, Z.C., (2009), "Removal behavior of Zn, Pb, K and Na from cold bonded briquettes of metallurgical dust in simulated RHF", *ISIJ Int.*, **49(12)**, 1874-1881.

COETSEE, T., PISTORIUS, P.C. and VILLIERS, E.E., (2002), "Rate-determining steps for reduction in magnetite-coal pellets", *Miner. Eng.*, **15**, 919-929.

DONSKOI, E. and MCELWAIN, D.L.S., (2001), "Mathematical modelling of non-isothermal reduction in highly swelling iron ore–coal char composite pellet", *Ironmak. Steelmak.*, **28**, 384-389.

FORTINI, O.M. and FRUEHAN, R.J., (2005), "Rate of reduction of ore-carbon composites: Part II. Modeling of reduction in extended composites", *Metall. Mater. Trans. B*, **36B**, 709-717.

SUN, K. and LU, W.K., (2009), "Mathematical modeling of the kinetics of carbothermic reduction of iron oxides in ore-coal composite pellets", *Metall. Mater. Trans. B*, **40(1)**, 91-103.

SUN, K. and LU, W.K., (1999), "Building of a mathematical model for the reduction of iron ore in ore/coal composites", *ISIJ Int.*, **39(2)**, 130-138.

SUN, K. and LU, W.K., (1993), "Mathematical modelling of reactions in iron ore/coal composites", *ISIJ Int.*, **33(10)**, 1062-1069.

WU, Y.L., JIANG, Z.Y., ZHANG, X.X., WANG, P. and SHE, X.F., (2013), "Numerical simulation of the direct reduction of pellets in a rotary hearth furnace for zinc-containing metallurgical dust treatment", *Int. J. Miner. Metall. Mater.*, **20(7)**, 636-644.

LIU, Y., WEN, Z., LOU, G.F., LI, Z., YONG, H.Q. and FENG, X.H., (2014), "Numerical Investigation of the Effect of C/O Mole Ratio on the Performance of Rotary Hearth Furnace Using a Combined Model", *Metall. Mater. Trans. B*, **45(6)**, 2370-2381.

HUA, Y.X., (2003), "Introduction to Kinetics of Metallurgy Process", *Metallurgical Industry Press, Beijing*, 162-165.